Environ. Sci. Technol. **2006**, *40,* 2045−2050

Arsenic(V) Removal from Groundwater Using Nano Scale Zero-Valent Iron as a Colloidal Reactive Barrier Material

SUSHIL RAJ KANEL,[†] JEAN-MARK GRENECHE,[‡] AND HEECHUL CHOI*,[†]

Department of Environmental Science and Engineering, Gwangju Institute of Science and Technology (GIST), 1 Oryong-dong, Buk-gu, Gwangju 500-712, Korea, LPEC, UMR 6087 CNRS, Université du Maine, avenue Olivier Messiaen, 72085 Le, Mans Cedex 9, France

The removal of As(V), one of the most poisonous groundwater pollutants, by synthetic nanoscale zero-valent iron (NZVI) was studied. Batch experiments were performed to investigate the influence of pH, adsorption kinetics, sorption mechanism, and anionic effects. Field emission scanning electron microscopy (FE−SEM), high-resolution transmission electron microscopy (HR−TEM), X-ray diffraction (XRD), X-ray photoelectron spectroscopy (XPS), and Mössbauer spectroscopy were used to characterize the particle size, surface morphology, and corrosion layer formation on pristine NZVI and As(V)-treated NZVI. The HR−TEM study of pristine NZVI showed a core-shell-like structure, where more than 90% of the nanoparticles were under 30 nm in diameter. Mössbauer spectroscopy further confirmed its structure in which 19% were in zero-valent state with a coat of 81% iron oxides. The XRD results showed that As(V)-treated NZVI was gradually converted into magnetite/maghemite corrosion products over 90 days. The XPS study confirmed that 25% As(V) was reduced to As(III) by NZVI after 90 days. As(V) adsorption kinetics were rapid and occurred within minutes following a pseudo-first-order rate expression with observed reaction rate constants (k_{obs}) of 0.02−0.71 min^{-1} at various NZVI concentrations. Laser light scattering analysis confirmed that NZVI−As(V) forms an inner-sphere surface complexation. The effects of competing anions revealed that HCO_3^-, $H_4SiO_4^0$, and $H_2PO_4^{2-}$ are potential interfering agents in the As(V) adsorption reaction. Our results suggest that NZVI is a suitable candidate for As(V) remediation.

Introduction

Recognized as a highly toxic element, arsenic (As) is abundant in our environment with both natural and anthropogenic sources (*1*). It is present in a variety of forms, organic and inorganic, and oxidation states, in which the valances depend on the pH and redox conditions (*1*, *2*). Arsenic contamination has aroused attention due to groundwater levels in many parts of the world at much higher concentrations than the World Health Organization (WHO) guideline of 10 μg/L (*3*). This situation has become more serious due to increasing groundwater consumption in many countries such as Bangladesh, West Bengal (India), and Nepal in the Indo region due to resource pressures from growing populations as well as surface water contamination (*1*, *4*).

The predominant forms of arsenic in groundwater and surface water are the inorganic species arsenate [As(V)] and arsenite [As(III)]. The As(V) species exists as oxyanions ($H_2AsO_4^{1-}$ and $HAsO_4^{2-}$) at neutral pH, whereas the As(III) species remains protonated as $H_3AsO_3^0$ at pH below 9.2 (*5*, *6*). Moreover, the formation of As(III) species is favored in soil and groundwater with low redox potential whereas As(V) exists at a redox potential above 100 mV and in an oxidizing environment (*6*).

Recently, zero-valent iron (ZVI) has become one of the most common adsorbents for the rapid removal of As(III) and As(V) in the subsurface environment (*7*−*13*). Significantly, the reactivity of ZVI has recently been improved by the development of smaller sized, zero-valent iron, i.e., nanoscale zero-valent iron (NZVI). Its application to remove varieties of pollutants has been demonstrated with halogenated hydrocarbons such as TCE, PCE (*14*−*17*), carbon tetrachloride (*18*), anions (e.g., NO_3^-, $Cr_2O_7^{2-}$), heavy metals (e.g., Ni^{2+}, Hg^{2+}), radio-nuclides (*19*), As(III) (*20*) and organic compounds such as benzoic acid (*21*). Hence, it has been proposed to use this material as a colloidal reactive barrier for in situ groundwater remediation (*22*, *23*).

In this paper, we report our investigation of As(V) remediation using NZVI studied by different spectroscopic and microscopic techniques. Furthermore, we confirmed the finding that As(V) can be reduced into As(III) by NZVI. Time-resolved study using field emission scanning electron microscopy (FE−SEM), X-ray photoelectron spectroscopy (XPS), Mössbauer spectrometry, and X-ray diffraction (XRD) showed structural, morphological, and chemical changes of As(V) and NZVI up to 3 months. The main objectives of our research are (i) to characterize NZVI and its reaction products before and after their reaction with As(V), (ii) to delineate the kinetics of As(V) sorption, (iii) to understand the sorption mechanisms by combining different microscopic and spectroscopic studies, (iv) to investigate the anionic competitive effects, and (v) to test the potential of NZVI for As(V) removal using field-collected groundwater from Bangladesh and West Bengal (India).

Experimental Methods

Materials and Chemicals. The chemical reagents used in the study ($NaAsO_2$, $Na_2HAsO_4{\cdot}7H_2O$, HCl, NaOH, NaH_2PO_4, KI, and $NaBH_4$) were reagent grade obtained from Aldrich Chemical Co. or Fluka Chemical Co. In some experiments, groundwater from Bangladesh (*24*) and West Bengal (India) (pH, total alkalinity, dissolved organic carbon, sulfate, and phosphate of the groundwater were 6.5, 319.7 mg/L, 1.0 mg/L, 8.5 mg/L ,and 0.09 mg/L, respectively) were used. NZVI were synthesized as described in our previous report (*20*). The pristine NZVI and As(V)-treated NZVI material were characterized by high-resolution transmission electron microscopy (HR−TEM), XRD, field emission SEM (FE−SEM), Mössbauer spectroscopy, XPS, laser light scattering, and the Brunauer−Emmett−Teller (BET) equation. Philips CM 20 was used for HR−TEM with an accelerated voltage of 200 keV. Mössbauer spectra were carried out at 4.2, 77, and 300 K using a spectrometer with a triangular waveform and a source of ^{57}Co (50 mCi). The hyperfine parameters (H_{hf}, hyperfine field; IS, isomer shift; QS, quadrupolar splitting;

* Corresponding author phone: +82−62−970−2441; fax: +82−62−970−2434; e-mail: hcchoi@gist.ac.kr.
† Gwangju Institute of Science and Technology (GIST).
‡ Université du Maine.

10.1021/es0520924 CCC: $33.50
Published on Web 02/11/2006

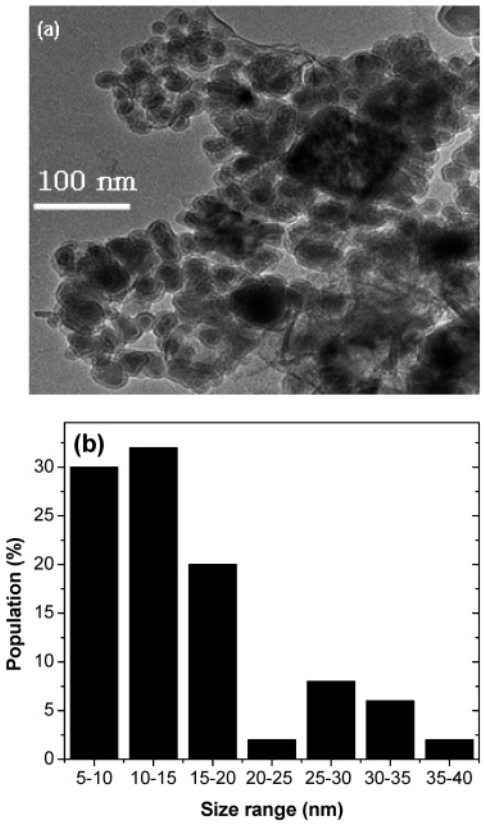

FIGURE 1. TEM image of pristine NZVI (a) and its Histogram (b).

2ϵ, quadrupolar shift; line width at half-height; %, ratio of each component; standard deviations: ± 0.02 mm s^{-1} and $\pm 3\%$) were refined using a least-squares fitting procedure in the MOSFIT program (*25*). XPS analysis was performed on a Physical Electronics 5500/5600 ESCA system with monochromatic Al Kα radiation (1486.7 eV) as X-ray source. Further details about other analytical methods and procedures for As(V) adsorption/desorption studies can be found in our previous report (*20*).

Results and Discussion

Microscopic and Spectroscopic Studies. HR−TEM was used to investigate the morphology and size distribution of pristine NZVI. Figure 1 shows clearly two distinct layers as a core−shell-like, structural domain, where the shell (thickness of ~10 nm) is probably due to iron oxide(s) while the core (~20 nm diameter) is attributed to Fe^0. Statistical calculation by histogram established from the TEM images confirmed that >92% of the nanoparticles were under 30 nm diameter (Figure 1b). However, they formed a chainlike, aggregated structure because of the natural tendency to remain in the more thermodynamically stable state (*26*) during oxidation and corrosion to Fe(III) oxide/hydroxide.

To test the longevity of the colloidal reactive barrier material, the NZVI was reacted with 20 mL of 100 mg L^{-1} As(V) for different time periods (0, 7, 30, 60, and 90 days). The reaction products were collected by freeze-drying, and were analyzed in powder mode by microscopic and spectroscopic techniques. The morphological appearances of the pristine NZVI and As(V)-treated NZVI shown by FE−SEM are presented in Figure 2. The images show different surface textures and pore sizes according to the time of adsorption/precipitation of As(V) onto NZVI. Pristine NZVI has a pore size of 20 nm and a specific surface area of 25 m^2/g, as measured by BET. The SEM image shows that ~90% of the pristine NZVI (round shape attached on hexagonal iron oxide) were initially within the ~1−50 nm size range (Figure 2a). The appearance of the slightly larger size in the SEM image than in the HR−TEM image is due to the difference in resolution of the two independent analytical techniques. However, the morphology of these NZVI changed further during the 7-day reaction (Figure 2b), as evidenced by the appearance of magnetite/maghemite and lepidocrocite and by the disappearance of the Fe^0 peak with increased amorphous region (Figure 3b), in comparison with that of pristine NZVI (Figure 3a) as shown in XRD.

Similar phenomena were observed in the time-resolved XRD result of As(III)-treated NZVI for 7 days (*20*). Interestingly, the amorphous region had almost disappeared at 30 days and sharp crystalline peaks of lepidocrocite and magnetite/maghemite are seen (Figure 3c). After 60 days, the main corrosion products were magnetite/maghemite, whereas the lepidocrocite had completely disappeared (Figure 3d). The same trend is evident in the 90-day product but, interestingly, the amorphous phase at 15−35 (2-theta) has been increased (Figure 3e). The SEM picture clearly shows the growth of chainlike aggregates on the 60-day samples (Figure 2c), and these aggregates became more distinct in the 90-day sample (Figure 2d). However, in case of As(III)-treated NZVI, only round-shape aggregated particles were seen even after 60 days (*20*). However, XRD presented a new peak at 82 (2-theta degree) in the 60−90-day samples (Figure 3d,e), which may be attributed to As(V) adsorbed Fe^0, which was not observed in the case of As(III)-treated NZVI (*20*).

To understand the dynamic characteristics over time of NZVI in the presence of As(V), Mössbauer spectroscopy was conducted. Figure 4 presents a comparison of the Mössbauer spectra of ZVI (Kanto Chemical Company, Japan), NZVI and As(V)-treated NZVI. ZVI (Figure 4a) showed a single magnetic component corresponding to Fe^0. The hyperfine parameters were nicely consistent with those of the body centered, cubic phase of metallic Fe (bcc−Fe). No satellite lines were observed, indicating that the quantity of iron oxide was quite small (<2% taking into account the detection limit). For the pristine NZVI (Figure 4b) a quite complex hyperfine structure is seen. At least five components are distinguishable: the magnetic sextet with narrow lines corresponds to that of Fe^0 (~19% in terms of Fe nuclei), two quadruple components which are due to Fe^{3+} and Fe^{2+} species, and two magnetic components. Taking the previous results into consideration (*27*, *28*), the Mössbauer spectra suggested the presence of disordered ferric oxide and/or superparamagnetic ferric oxide on the surface due to the passivation of metallic Fe, with a broad distribution of thicknesses. The pink and cyan colored components corresponded to magnetically blocked and superparamagnetic Fe oxide particles, respectively. In addition, there was a divalent Fe quadruple component (green colored) which can be assigned to $Fe(OH)_2$. Similar results were observed during the synthesis of NZVI, where 28% of Fe^0 was coated with 72% of iron oxide in the presence of oxygen (*27*).

Similarly for the 7-day sample (Figure 4c), a quadruple component and a magnetic sextet with broadened lines were observed, which were attributed to ferric species. It is important to emphasize that the metallic Fe (Fe^0) phase did not exceed 1% at this stage. The quadruple doublet was unambiguously attributed to the lepidocrocite (~30%) while the sextet was assigned to a mixture of maghemite. For the 90-day sample (Figure 4d), there was a prevailing sextet with rather narrow lines, which unambiguously corresponded to metallic Fe (~42%) and a quadruple doublet in the central part; the hyperfine parameters did not strongly differ from those of lepidocrocite. This increase in Fe^0 content corroborated with the XRD results (Figure 3), where a new Fe^0 peak was observed after 60 days of reaction. In this study, we have quantified, for the first time, the different forms of

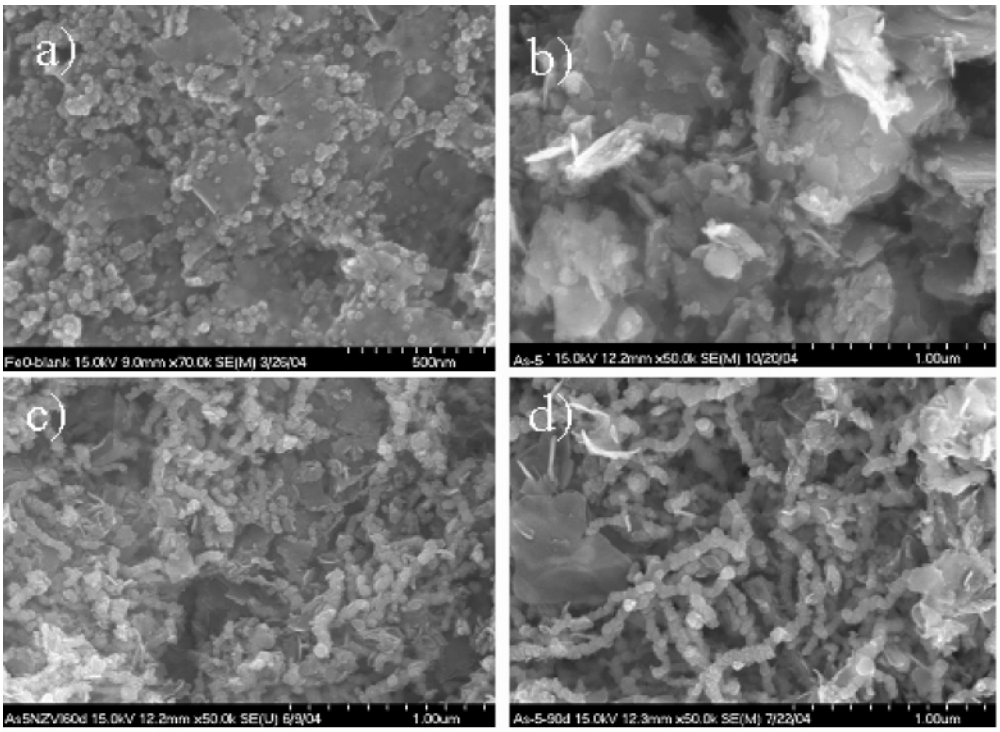

FIGURE 2. SEM images of (a) pristine NZVI, and (b), (c), and (d) are 100 mg/L As (V) adsorbed on 50 g/L NZVI in 0.01 M NaCl at pH 7, 25 °C, for 7, 60, and 90 days, respectively.

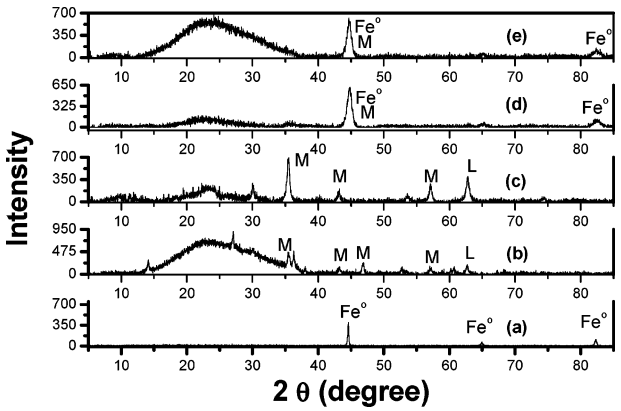

FIGURE 3. X-ray diffraction analysis of pristine NZVI (a) and 100 mg/L As (V) adsorbed on 50 g/L NZVI in 0.01 M NaCl at pH 7, 25 °C, for 7 days (b), 30 days (c), 60 days (d), and 90 days (e). The peaks are due to magnetite-maghemite (Fe_3O_4/γ-Fe_2O_3) and lepidocrocite (γ-FeOOH). Peaks are referred to magnetite/maghemite (M) (Fe_3O_4/γ-Fe_2O_3/), lepidocrocite (γ-FeOOH) (L), and NZVI (Fe°).

Fe present in As(V)-treated NZVI, and have confirmed the change over time of the percentage of zero-valent state iron.

Similarly, to test the valence state of As, NZVI treated with As(V) at different reaction times of 1, 7, 60, and 90 days were analyzed by XPS in powder mode (Figure 5). Until 60 days, only As(V) was detected, but notably in the 90-day sample, 25% of As(III) was identified due to the reduction of As(V). Similar results were reported in closed batch reactors during the reduction of As(V) by micron ZVI due to the formation of Fe(II) and Fe(III), or the formation of H_2 gas, which may have reduced the redox potential of the solution favoring As(V) reduction (*8*, *29*). On the other hand, very little or no reduction of As(V) by ZVI has also been reported in the case of opened reactors (*10*).

As(V) Removal. The effect of pH (*3*−*11*) on the adsorption of As (V) (1 mgL^{-1}) on NZVI (0.1 g/L) was studied (Figure 6). The 100% sorption of As_T (total arsenic) at pH 3−7 was

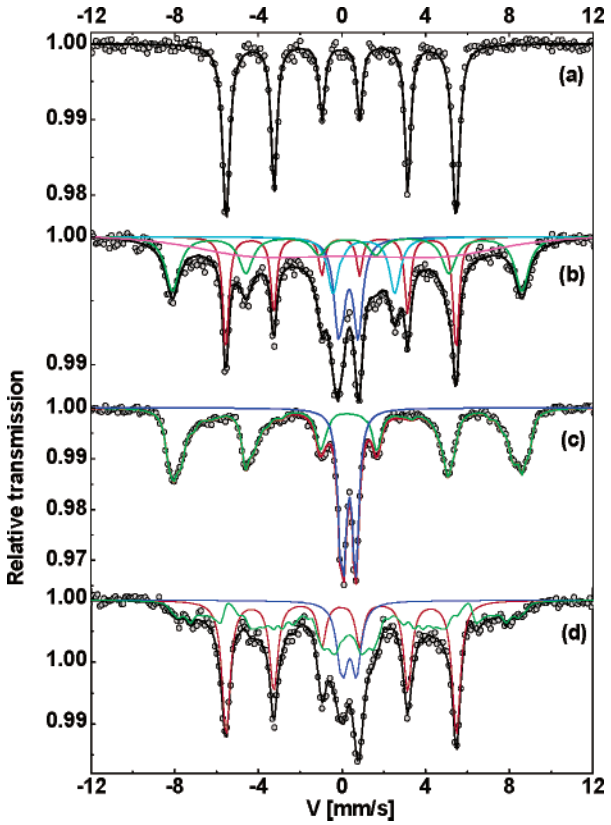

FIGURE 4. Mössbauer spectrum of ZVI from Kanto Chemical Company (Japan) (a), pristine NZVI (b) and 100 mg/L As (III) adsorbed on 50 g/L NZVI in 0.01 M NaCl for 7 days (c) and 90 days (d).

decreased to ~84.7% at pH 9 and ~37.9% at pH 11. This shows that NZVI is effective in acidic and neutral pH, which is analogous to our previous report on the sorption of As(III) by NZVI (*20*). Similarly, this trend of a pH dependence of As(V) was also observed during As removal by different iron

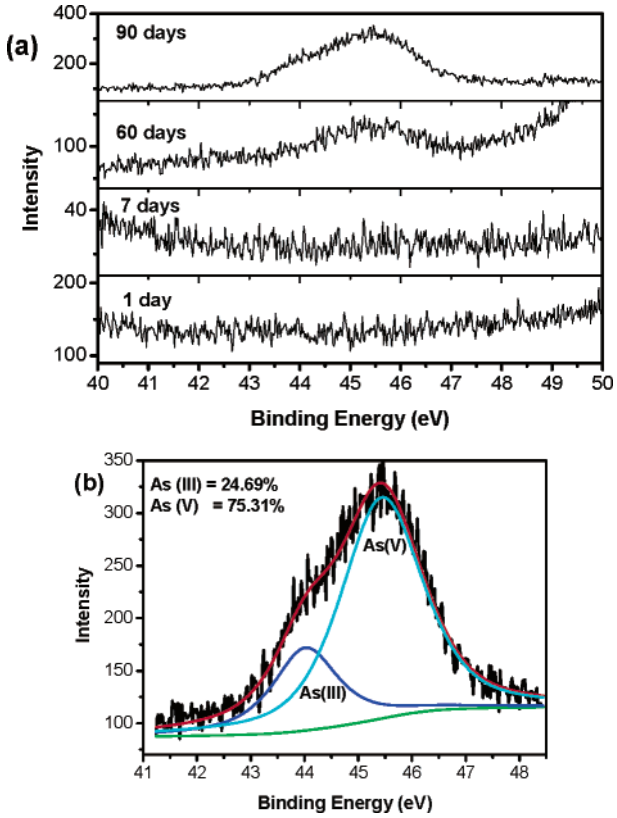

FIGURE 5. X-ray photoelectron spectroscopy of NZVI with 100 mg/L As (V) adsorbed on 50 g/L NZVI in 0.01 mM NaCl for 7, 60, and 90 days (a). Curve fitting of 90 days As(V)-treated NZVI product led to two distinct peaks, where 75.31% is As (V) and 24.69% is As (III) (b).

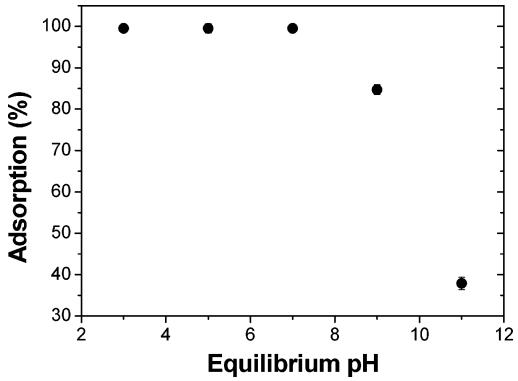

FIGURE 6. Adsorption of As(V) on NZVI as a function of pH. Reaction condition: 1 mgL^{-1} As(V) adsorbed on 0.1 gL^{-1} NZVI in 0.01M NaCl for a reaction time of 12 h. Ambient pH = 6.5 and was adjusted with 1M HCl or NaOH.

oxides (*30*) which may be attributed to the ionization of both adsorbates and adsorbents. As(V) has pK_1, pK_2, and pK_3 values of 2.2, 7.08, and 11.5, respectively. In the pH range of 2−7, $H_2AsO_4^-$ and $HAsO_4^{2-}$ are the predominant species of As (*31*), and are presumably the major species being adsorbed. As the iso−electric point (IEP) of NZVI is pH 7.7 (*20*), the NZVI surface exhibits a net positive charge at pH lower than pH 7.7 and the adsorption of trace anionic As (V) species was enhanced by columbic interaction. However, as the 0.1 and 1 mg/L concentrations of As(V) were added onto 0.1 g/L NZVI, the IEP of NZVI was decreased from 7.7 to ~7.5 and 7.2, respectively, indicating that As(V) might have become attached on the NZVI corrosion product surface by forming inner sphere complexes (*7*, *20*, *32*).

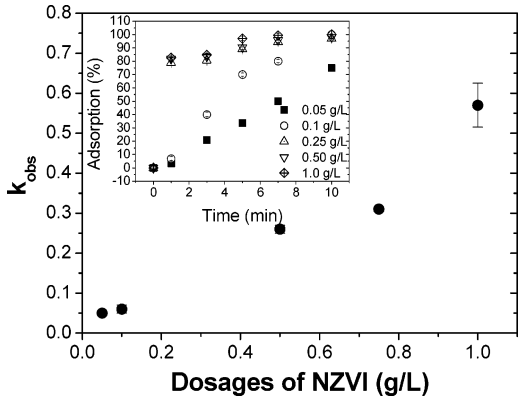

FIGURE 7. Effects of NZVI concentration on As (V) adsorption. The reaction is pseudo first order with respect to the total NZVI concentration, As (V): 1 mg/L, pH 7, 25 °C. Upper inset shows As(V) adsorption with respect to time; Initial As (V): 1 mg/L in 0.01 M NaCl, pH 7, 25 °C.

TABLE 1. Pseudo-First-Order Rate Constants (k_{obs}) and Their Surface Area Normalized Rate Constants (k_{sa}) for As(V) Removal by NZVI.[a]

NZVI (g/L)	k_{obs} (min^{-1})	k_{sa} (Lm^{2}min^{-1})	R^2
0.05	0.02	0.015	0.83
0.10	0.06	0.025	0.87
0.25	0.38	0.062	0.99
0.5	0.42	0.034	0.99
0.75	0.51	0.028	0.92
1.00	0.71	0.029	0.83

[a] As(V): 1 mg/L in 0.01 M NaCl at pH 7, 25 °C

The identity of the actual reactive surface site for As(V) removal may change over time, i.e., during the course of the reaction. The results of time-resolved XRD and Mössbauer spectroscopy suggested that initially (0−7 days) amorphous Fe(II)/(III), lepidocrocite, and magnetite (or maghemite) are the main sites for As(V) adsorption; by the 60−90 day period, this has changed to magnetite/maghemite with Fe^0. This confirms that the suite of available reactive sites for As(V) adsorption changes over time. In addition, the layers of As-(V) adsorbed on NZVI corrosion product films are buried by successive layers and become occluded from the surrounding solution in the same manner as that of As(III) sorption on NZVI (*20*).

Kinetics of As Adsorption. The As(V) adsorption kinetics were examined using different concentrations of NZVI in a 50-mL vial with an initial pH of 7 (Figure 7). The removal of As(V) was fitted to a pseudo-first-order reaction kinetics, as we reported before (*20*). The influence of NZVI concentrations (0.05, 0.25, 0.5, 0.75, 1.0 gL^{-1}) on the rate of adsorption of 1 mgL^{-1} concentration of As (V) is shown in Figure 7. The figure shows that about 90% As_T was adsorbed within 7 min (Figure 7 inset) and ~99.9% within 60 min. Interestingly, As(V) adsorption was increased with increasing the adsorbent concentration (0.05 to 1.0 g/L). This corresponds, with the increase in the adsorbent dose, to the increase in the number of active sites, which enhances the As(V) adsorption. Hence, the optimum NZVI concentration of 0.1 g/L, at which arsenic removal was maximized with minimum NZVI concentration, was used in all the experiments unless otherwise specified.

Comparison of As Removal by Micron ZVI and NZVI. To elucidate, in detail, the differences in As removal by micron ZVI and NZVI, we compiled, in table 2, our results with those from the literature. It is clearly seen from Table 2 that the surface area of ZVI increased from 1 to 2 m^2/g to 35 m^2/g in 8 months (*33*). On the other hand, the surface area of NZVI

TABLE 2. Comparison of As Removal by Micron and Nano ZVI

Fe^0 type	k_{sa}	S_i	S_f	experimental condition	result summary	ref
NZVI	1500	25.0		NZVI: 1 g/L As(V):1 mg/L batch study	~100% As(V) removal in 10 min	Q
NZVI	690	24.4	37.2	NZVI: 0.1 g/L As(III):1 mg/L batch study	~100% As(III) removal in 10 min	20
F, P, M, and A (micron ZVI)	F: 35.6 P: 0.57 M: 0.44 A: 1.15	F: 0.09 P: 2.53 M: 2.33 A: 0.19		ZVI: 24 g/L As(V)/As(III): 2 mg/L batch study	As(V) removal F>P~M>A ~100% As(III) removal in 96 h	8
C, M (micron ZVI)		C:1.9, M:1.0	C:>1.9 M:>1.0	As(III)/As(V) column study	95% removal	12
ZVI, C	1.9		37.8	As(III) column study	As(III) removal for 8 months < 10 μg/L	33
F (Fe^0 −100, Fe^0 −40, rust −100, rust −40)[a]				As(III)/As(V) batch study	As_T removal(%): Fe0−100: 88.3; Fe0−40: 99.8; rust-100: 62.2; rust-40: 98.2	7
iron wire				0.1 to 20 mg/L: As(V), glass electrochemical cell	~ 100% removal of As(V)	29

[a] Different corrosion products, A = Aldrich, C = Connelly−GPM, F = Fisher, M = Master Builder, P = Peerless, and Q = This study; k_{sa}= surface area normalized rate constant of As reacted with ZVI or NZVI ($mLm^{-2}h^{-1}$); q = sorption capacity of As on ZVI or NZVI (mg/g); S_i = surface area of ZVI or NZVI before reaction with As (m^2/g); S_f: final surface area of ZVI or NZVI after reaction with As(m^2/g).

increased from 24.4 m^2/g to 37.2 m^2/g within 12 h (*20*). Furthermore, As was removed by NZVI within minutes, whereas it took hours to days for micron ZVI (*8*). However, the reaction mechanism of As removal was similar in both cases, i.e., by adsorption and precipitation. Interestingly, for both adsorbents, oxidation occurred in case of As(III), whereas reduction took place for As(V) only after two months in closed batch reactors (*8*, *20*), and there was no reduction in the case of open batch reactors (*29*). In addition, the generation mechanism of the iron oxide precipitates (from amorphous to crystalline structure) and the aging process appears to be similar in the case of both NZVI and ZVI. The study of Su and Puls (*8*) on the sorption of As(V) by micron ZVI showed the surface normalized rate constant (k_{sa}) for As(V) was 35.6, 0.57, 0.44, and 1.15 mL m^2 h^{-1} for the corrosion products of Fisher, Peerless, Master Builder, and Aldrich, respectively, for 24 g/L ZVI. In our experiment, the k_{sa} for As(V) was 900, 1500, 3720, 2040, 1680, and 1740 mL m^2 h^{-1} at 0.05, 0.1, 0.25, 0.5, 0.75, and 1.0 g/L NZVI, respectively, indicating that k_{sa} of NZVI was 1−3 orders of magnitude higher than that of ZVI (Table 1). This outstanding reactivity of NZVI was presumed to be due to its much larger surface area.

Effect of Competing Anions. The effect of individual anions (HCO_3^-, SO_4^{2-}, NO_3^-, As(III), Si^{2+}, and PO_4^{3-}) on the adsorption of As (V) on NZVI was studied (Table 3). The HCO_3^-, SO_4^{2-}, and NO_3^- anions did not have a negative effect on the As(V) uptake up to a 1 mM concentration, whereas $H_4SiO_4^0$ and PO_4^{3-} (1 mM) reduced the uptake from 99.9% to 39.90, and 30.01%, respectively. However, when the concentration of anions was increased further to 10 mM, the adsorption of As (V) on NZVI decreased from 99% to 90, 98, and 79% for NO_3^-, SO_4^{2-} and HCO_3^-, respectively. However, $H_4SiO_4^0$ and PO_4^{3-} (10 mM) decreased the sorption of As(V) to 15.10% and 9.03%, respectively. On the other hand, these effects differed in the case of As(III) (*20*). The HCO_3^-, SO_4^{2-}, and NO_3^- anions at concentrations up to 10 mM had no effect on As(III) uptake, whereas $H_4SiO_4^0$ and $H_2PO_4^{2-}$ reduced its uptake from 99.9% to 44.94 and 66.3%, respectively (*20*). This result is very positive for in situ remediation due to the coexistence of several anions in groundwater. The decrease in adsorption in the presence of these anions is due to the competitive reaction with As (*9*, *34*, *35*).

TABLE 3. Percentage of As (V) Removal in the Presence of Competitive Anions[a]

anions, mM/μM	percentage uptake of As(V) in the presence of anion[b]					
	NO_3^- [c]	SO_4^{2-} [c]	HCO_3^- [c]	$H_4SiO_4^0$ [c]	PO_4^{3-} [c]	As (III)[d]
0.00	99.90	99.90	99.90	99.90	99.90	99.90
0.1	99.90	99.9	99.9	99.90	99.9	99.90
1.0	90.00	98.00	99.00	39.90	30.01	99.90
10.0	90.00	98.00	79.00	15.10	9.03	99.90

[a] Initial As (V): 1 mg/L, NZVI: 0.1 g/L in 0.01M NaCl, pH: 7, 25 °C. [b] Note: Percentage uptake of As(V) in the presence of anions: $n = 3$, average of triplicate results where the standard deviation is less than 5%. [c] Anions in mM. [d] Anions in μM.

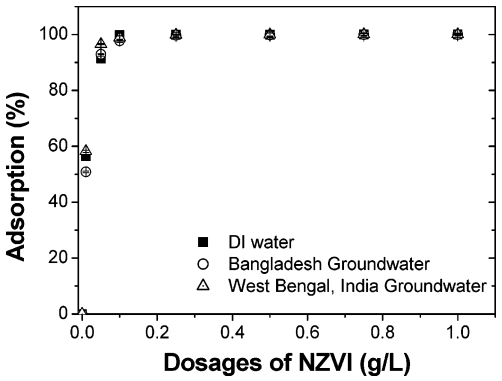

FIGURE 8. Sorption of As(V) using NZVI for Bangladesh and West Bengal (India) groundwater samples; As (V): 1 mg/L in 0.01 M NaCl, NZVI: 0.1 g/L, pH 7, 25 °C.

Application for the Removal of As from Groundwater. Batch studies on the removal of As (Figure 8) were carried out with groundwater samples obtained from Bangladesh and West Bengal, India. The total iron concentration of groundwater from both sources was 10 mg/L. As(V) was spiked in both samples to obtain an initial As(V) concentration

of 1 mg/L and its effect was studied using NZVI. As(V) was removed, with an efficiency reaching 100%, by 0.1, 0.2, and 0.4 g/L NZVI for the spiked DI water, and Bangladesh and West Bengal groundwater samples, respectively. A high amount of NZVI was required for complete removal of As(V) from the real groundwater samples, possibly due to the presence of dissolved organic carbon, sulfate, and phosphate in the real groundwater samples. These results confirm that NZVI could be used for removing As in countries of the Indo region, where groundwater is severely contaminated by As. We have presented evidence that As (V) can be removed by adsorption/precipitation on NZVI (at neutral pH) in a relatively short time of only several minutes. As(V) strongly adsorbs on NZVI over a wide pH range, through the coprecipitation of various iron oxide corrosion products. Finally, the study results presented here have confirmed the potential of NZVI as an efficient material for the treatment of As(V), and one that may be used as a permeable reactive barrier material for both in situ and ex situ groundwater remediation.

Acknowledgments

This work was supported by a grant from the National Research Laboratory Program operated by the Korea Science and Engineering Foundation. We are grateful to Professor Laurent Charlet (Environmental Geochemistry Group, LGIT, University of Grenoble, France) for his input in scientific discussions.

Literature Cited

(1) Smedley, P. L.; Kinniburgh, D. G. A review of the source, behaviour and distribution of Arsenic in natural waters. *Appl. Geochem*. **2002**, *17*, 517−568.
(2) Ferguson, J. F.; Gavis, J. Review of the arsenic cycle in natural waters. *Water Res.* **1972**, *6*, 1259−1274.
(3) WHO. *Guidelines for drinking water quality, Vol 1: Recommendations*. 2nd ed.; World Health Organization: Geneva. 1993.
(4) Kanel, S. R.; Choi H.; Kim, K. W.; Moon, S. H. Arsenic contamination in groundwater in Nepal: a new perspective and health threat in South Asia. In *Natural Arsenic in Groundwater: Occurrence, remediation and management;* Bundschuh, J., Bhattacharya P., and Chandrasekharam D., Eds.; Taylor and Francis (Balkema): London, 2005; pp 103−108.
(5) Oremland, R. S.; Stolz, J. F. The ecology of arsenic. *Science* **2003**, *300*, 393−944.
(6) Korte, N. E.; Fernando, Q. A review of arsenic(III) in groundwater. *Crit. Rev. Environ. Control* **1991**, *21*, 1−39.
(7) Manning, B. A.; Hunt, M.; Amrhein, C.; Yarmoff, J. A. Arsenic-(III) and arsenic(V) reactions with zerovalent iron corrosion products. *Environ. Sci. Technol*. **2002**, *36*, 5455−5461.
(8) Su, C.; Puls, R. W. Arsenate and arsenite removal by zerovalent iron: Kinetics, redox transformation, and implications for in situ groundwater remediation. *Environ. Sci. Technol*. **2001**, *35*, 1487−1492.
(9) Su, C.; Puls, R. W. Arsenate and arsenite removal by zerovalent iron: Effects of phosphate, silicate, carbonate, borate, sulfate, chromate, molybdate, and nitrate, relative to chloride. *Environ. Sci. Technol*. **2001**, *35*, 4562−4568.
(10) Farrell, J.; Wang, J.; O'Day, P.; Coklin, M. Electrochemical and spectroscopic study of arsenate removal from water using zerovalent iron media. *Environ. Sci. Technol*. **2001**, *35*, 2026−2032.
(11) Leupin, O. X.; Hug, S. J. Oxidation and removal of arsenic (III) from aerated groundwater by filtration through sand and zerovalent iron. *Water Res.* **2005**, *39*, 1729−1740.
(12) Lackovic, J. A.; Nikolaids, N. P.; Dobbs, G. M. Inorganic arsenic removal by zerovalent iron. *Environ. Eng. Sci.* **2000**, *17*, 29−39.
(13) Bang, S.; Johnson, M. D.; Korfiatis, G. P.; Meng, X. Chemical reactions between arsenic and zero-valent iron in water. *Water Res.* **2005**, *39*, 763−770.
(14) Wang, C. B.; Zhang, W. Synthesizing nanoscale iron particles for rapid and complete dechlorination of TCE and PCBs. *Environ. Sci. Technol.* **1997a**, *31*, 2154−2156.
(15) Lien, H.-L.; Zhang, W. Transformation of chlorinated methanes by nanoscale iron particles. *J. Environ. Eng.* **1999**, *125*, 1042−1047.
(16) Schrick, B.; Blough, J. L.; Jones, A. D.; Mallouk, T. E. Hydrodechlorination of trichloroethylene to hydrocarbons using Bimetallic nickel−iron nanoparticles. *Chem. Mater.* **2002**, *14*, 5140−5147.
(17) Lowry, G. V.; Johnson, K. M. Congener-specific dechlorination of dissolved PCBs by microscale and nanoscale zerovalent iron in a water/methanol solution. *Environ. Sci. Technol.* **2004**, *38*, 5208−5216.
(18) Nurmi, J. T.; Tratnyek, P. G.; Sarathy, V.; Baer, D. R.; Amonette, J. E.; Pecher, K.; Wang, C.; Linehan, J. C.; Matson, D. W.; Penn, R. L.; Driessen, M. D. Characterization and properties of metallic iron nanoparticles: spectroscopy, electrochemistry, and kinetics. *Environ. Sci. Technol.* **2005**, *39*, 1221−1230.
(19) Zhang, W. X. Nano scale iron particles for environmental remediation: an overview. *J. Nanopart. Res.* **2003**, *5*, 323−332.
(20) Kanel, S. R.; Manning, B.; Charlet, L.; Choi, H. Removal of arsenic-(III) from groundwater by nano scale zero-valent iron. *Environ. Sci. Technol.* **2005**, *39*, 1291−1298.
(21) Joo, S. H.; Feitz, A. J.; Sedlak, D. L.; Waite, T. D. Quantification of the oxidizing capacity of nanoparticulate zerovalent iron. *Environ. Sci. Tech.* **2005**, *39*, 1263−1268.
(22) Elliot, D. W.; Zhang, W. X. Field assessment of nanoscale bimetallic particles for groundwater treatment. *Environ. Sci. Technol.* **2001**, *35*, 4922−4926.
(23) Cantrell, K. J.; Kaplan, D. I. Zero-valent iron colloid emplacement in sand columns. *J. Environ. Eng.* **1997**, *123*, 499−505.
(24) Mukherjee, A. B.; Bhattacharya, P. Arsenic in groundwater in the Bengal delta plain: slow poisoning in Bangladesh. *Environ. Rev.* **2001**, *9*, 189−220.
(25) Sanselme, M.; Grenèche, J.-M.; Riou-Cavellec, M.; Férey, G. The first ferric carboxylate with a three-dimensional hydrid open-framework (MIL-82): its synthesis, structure, magnetic behavior and study of its dehydration by Mössbauer spectroscopy. *Solid State Sci.* **2004**, *6*, 853−858.
(26) Cushing, B. L.; Kolesnichenko, V. L.; O'Connor, C. J. Recent advances in the liquid-phase syntheses of inorganic nanoparticles. *Chem. Rev.* **2004**, *104*, 3893−3946.
(27) Bianco, L. D.; Fiorani, D.; Testa, A. M.; Bonetti, E.; Savini, L. Magnetothermal behaviour of a nanoscale Fe/Fe oxide granular system. *Phys. Rev.* **2002**, *66*, 174418−1−174418−11.
(28) Rojas, T. C.; Sanchez-Lopez, J. C.; Grenèche, J. M.; Conde, A.; Fernandez, A. Characterization of oxygen passivated iron nano particles and thermal evolution to r-Fe2O3. *J. Mater. Sci*. **2004**, *39*, 4877−4885.
(29) Melitas, N.; Conklin, M.; Farrell, J. Electrochemical study of arsenate and water reduction of iron media used for arsenic removal from potable water. *Environ. Sci. Technol.* **2002**, *36*, 3188−3193.
(30) Dixit, S.; Hering, J. G. Comparison of arsenic(V) and arsenic(III) sorption onto iron oxide minerals: Implications for arsenic mobility. *Environ. Sci. Technol.* **2003**, *37*, 4182−4189.
(31) Kartinen, E. O.; Martin, C. J. An overview of arsenic removal processes. *Desalination* **1995**, *103*, 79−88.
(32) Goldberg; Johnston, 2001, Mechanism of arsenic adsorption on amorphous oxides evaluated using macroscopic measurements, vibrational spectroscopy, and surface complexation modeling. *J. Colloid Interface Sci. 234*, 204−216.
(33) Nikolaidis, N. P.; Dobbs, G. M.; Lackovic, J. A. Arsenic removal by zero-valent iron: field, laboratory and modeling studies. *Water Res.* **2003**, *37*, 1417−1425.
(34) Cheng, Z.; Van Geen, A.; Louis, R.; Nikolaidis, N.; Bailey, R. Removal of methylated arsenic in groundwater with iron filings. *Environ. Sci. Technol.* **2005**, *39* (19), 7662−7666.
(35) Radu, T.; Subacz, J. L.; Phillippi, J. M.; Barnett, M. O. Effects of Dissolved Carbonate on Arsenic Adsorption and Mobility. *Environ. Sci. Technol.* **2005**, *39* (20), 7875−7882.

Received for review October 21, 2005. Revised manuscript received December 31, 2005. Accepted January 11, 2006.

ES0520924